Preliminary analysis of an *in-situ* measurement system for normal-incidence absorption coefficient using a microphone array

Paolo Bonfiglio[a]* | Daniele Ponteggia[a] | Andrea Farnetani[a]

[a] Materiacustica Srl,
Via Ravera, 15A, 44122 Ferrara
* Corresponding author:
paolo.bonfiglio@materiacustica.it

Ricevuto: 17/1/2026
Accettato: 17/3/2026

DOI: 10.3280/riaof-2026oa21889
ISSNe: 2385-2615

Acoustic characterization of materials is crucial to evaluate their sound-absorbing properties under real conditions. Standard methods, such as the impedance tube (ISO 10534-2) and the re-verberation chamber (ISO 354), show limitations for *in-situ* measurements. This study presents an innovative approach to estimate the normal-incidence absorption coefficient using a low-cost 4×4 microphone array. The method computes normalized acoustic impedance and reflection coefficient from microphone pairs, with free-field calibration. The system covers 100 Hz-5000 Hz through variable spacers and reduces operational complexity compared to traditional techniques. Numerical validation via finite element modelling and experimental tests in anechoic chamber show good agreement with analytical models and standards, with deviations comparable to the reproducibility of standardized methods. Results confirm the robustness of the approach against geometric variations and edge effects, enabling fast and reliable measurements in real environments.
Keywords: materials characterization, normal-incidence absorption coefficient, microphone array, acoustic impedance

Analisi preliminare di un sistema di misura *in situ* per il coefficiente di assorbimento a incidenza normale mediante array di microfoni
La caratterizzazione acustica dei materiali è cruciale per valutarne le proprietà fonoassorbenti in condizioni reali. I metodi standard, come il tubo d'impedenza (ISO 10534-2) e la camera riverberante (ISO 354), mostrano limiti nelle misure in situ. Questo studio propone un approccio innovativo per stimare il coefficiente di assorbimento a incidenza normale mediante un array di microfoni a basso costo (4×4). La tecnica si basa sul calcolo di impedenza acustica normalizzata e coefficiente di riflessione da coppie di microfoni, con calibrazione in campo libero. Il sistema copre 100 Hz-5000 Hz grazie a distanziatori variabili e riduce la complessità rispetto alle procedure tradizionali. La validazione numerica, tramite elementi finiti, e le prove in camera anecoica evidenziano buona concordanza con modelli analitici e standard, con scarti medi in linea con la riproducibilità delle tecniche normate. I risultati confermano la robustezza del metodo rispetto a variazioni geometriche ed effetti di bordo, aprendo la strada a misure rapide e affidabili in ambienti reali.
Parole chiave: caratterizzazione materiali, coefficiente di assorbimento per incidenza normale, array microfonico, impedenza acustica

1 | Introduction

Acoustic characterization of materials represents the starting point for evaluating their sound-absorbing and reflecting properties. Traditionally, this phase relies on standardized laboratory methods, which ensure repeatability, more robust comparison among samples tested by different laboratories, and compliance with international regulations.

One of the most commonly adopted techniques in acoustic characterization is the impedance tube method, standardized by ISO 10534-2 [1] and ASTM E1050 [2]. This approach allows the determination of the normal-incidence absorption coefficient and the surface impedance, Z_s, of the material. This technique is based on measuring the transfer function between two microphones mounted inside a rigid tube through which the sound wave propagates. This method offers several advantages: it is fast, requires small samples of material, and directly provides the value of Z_s. However, it does not reproduce the diffuse-field conditions typical of real environments and therefore may not always represent in-situ performance. A second well-established method is the reverberation chamber technique, described in ISO 354 [3] and ASTM C423 [4]. In this case, the absorption coefficient is estimated under diffuse-field conditions by exploiting the variation in sound decay times with and without the sample inside the chamber. This technique is particularly suitable for defining product specifications under diffuse field conditions and for comparative assess-

ments on large samples. Nevertheless, it presents some critical issues: edge effects and diffraction phenomena may occur, and inconsistent results may be found due to simplified assumptions of the method, as in the case of highly absorbing materials for which absorption coefficient greater than unity can be found. When moving to in-situ measurements, several families of methods come into play to determine the absorption coefficient, α, the reflection coefficient, R, and the surface impedance, Z_s, under real conditions. Among these, the Tamura method deserves mention: it is based on measuring the complex acoustic field on two parallel planes close to the surface. Through a spatial Fourier transform, it is possible to separate the incident and reflected components, thus obtaining R for oblique incidences and deriving α and Z_s [5-8]. Other advanced techniques exploit microphone arrays and Near-Field Acoustic Holography (NAH), enabling reconstruction of the sound field near the surface and detailed estimation of Z_s and α, even as the incidence angle varies. Common configurations include double-layer arrays, spherical arrays, and approaches based on beamforming or adaptive nulling [9-13]. Another category of instruments is represented by pressure-velocity probes, which simultaneously measure pressure, p, and particle velocity, u, a few centimetres from the surface. This allows direct computation of surface impedance $Z_s = p/u$ and, consequently, R and α [14-16]. Two-microphone in-situ methods estimate normal impedance Z_s from their transfer function, H_{ab}, even in the presence of ambient noise. Variants, such as ensemble averaging, extend the measurement to random incidence and, more recently, have been integrated with data-driven approaches based on machine learning techniques [17-19]. Finally, in outdoor and road contexts, impulsive and subtraction methods are used, formalized by ISO 13472 (both the extended surface and spot methods). These approaches enable in-situ measurements on pavements and noise barriers, ensuring robustness to noise and compliance with standards [20-23]. A summary of the main advantages and disadvantages of the discussed methods is provided in Table 1.

The research presented here proposes a preliminary analysis of an innovative system for measuring the acoustic absorption coefficient under normal-incidence conditions, performed directly in-situ. The method is based on the use of a low-cost microphone array arranged in a 4×4 configuration, designed to ensure ease of implementation and cost reduction compared to traditional solutions. The primary goal of the proposed technique is to enable rapid and reliable determination of the absorption coefficient over an extended frequency range, overcoming the typical limitations of standardized methodologies and commonly reported procedures in the literature. This approach aims to offer greater operational flexibility, reducing measurement complexity and expanding applicability in real-world contexts where test conditions do not always allow the use of conventional techniques.

Tab. 1 – Comparison between standard and in-situ methods for measuring α and Z_s

Confronto tra metodi standard in situ per la misura di α e Z

Method (standard/ref.)	*Advantages*	*Disadvantages*
Impedance tube (ISO 10534-2-ASTM/ E1050)[1,2]	Small sample; direct measurement of Z_s; high repeatability	Lateral constraint effects
Reverberation chamber (ISO 354/ ASTM C423)[3,4]	Realistic diffuse field; datasheet reference	Large samples; α>1 possible; edge/ diffraction effects
SFT (Tamura)[5-7]	Angular information; full estimation of $R/Z_s/\alpha$	Complex setup; leakage; spurious reflections
Array/NAH[9-13]	Spatial mapping; non-invasive; *in-situ*	Cost/complexity; sensitivity to noise/ positioning
p-u probe[14-16]	Direct measurement of Z_s; fast, portable	Critical calibration; challenging at low frequencies
Two-microphone in situ[17-19]	Simple set-up; usable with ambient noise	Plane-wave propagation assumption; low-frequency limitations;
Impulse ISO 13472[20-23]	Robust in real-world conditions; large surfaces; reference standard	Dependence on gating/geometry.

The structure of this article is as follows. Section 2 introduces the theoretical framework underlying the proposed method, providing a detailed description of the principles and assumptions guiding its formulation, and the measurement set-up. Section 3 presents the validation activities, which include both numerical simulations and experimental tests aimed at assessing the effectiveness and reliability of the method. Finally, the main conclusions are discussed, and future development perspectives are outlined.

2 | Materials and Methods

2.1 | Proposed methodology

With reference to Figure 1, consider an acoustic monopole placed near a flat reflecting surface located in the plane $z = 0$. The system is analysed in the context of sound propagation with specular reflection, with two observation points (microphones M1 and M2) positioned in space. The distance between the source S and the midpoint is denoted by r, while the distance between the mirrored source S′ and the midpoint is indicated by r'. The midpoint is located at a vertical distance d from the reference plane.

Moreover:

- γ denotes the angle of incidence with respect to the vertical (normal to the reference plane);
- δ denotes the angle between the source and the projection of the midpoint onto the reference plane.

- θ_0 is the angle between the source and the point of reflection;
- r_0 is the distance between the source and the projection of the midpoint onto the reference plane.

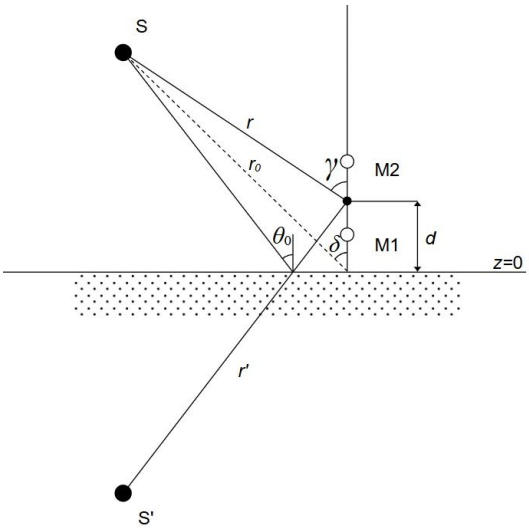

Fig. 1 – Geometry of the problem
Geometria del problema

The starting point of the proposed formulation (hereinafter referred to as the "Proposed methodology") is that the normalized acoustic impedance at the midpoint between two microphones can be calculated as:

$$z_M = \frac{1}{\rho c} \cdot \frac{p_M}{u_M} \; [-] \tag{1}$$

being:

$$p_M = \frac{p_{M1}+p_{M2}}{2} \; [Pa] \tag{2}$$

$$u_M = \frac{p_{M2}-p_{M1}}{j\rho c k a} \left[\frac{m}{s}\right] \tag{3}$$

the pressure and the particle velocity (in perpendicular direction to the reference plane) respectively and a is the distance between the microphones, k the wavenumber and c the speed of sound.

Starting from the normalized acoustic impedance at the midpoint, the complex reflection coefficient can be calculated as follows:

$$R(\theta_0) = \left(\frac{\beta\left(1+\frac{j}{kr}\right) z_M \cos(\theta_0) - 1}{\left(1+\frac{j}{kr}\right) z_M \cos(\theta_0) + 1}\right) \cdot \frac{r'}{r} \cdot e^{-ik(r-r')} \tag{4}$$

where β is calculated from Figure 1 as:

$$\beta = \frac{\cos(\gamma)}{\cos(\theta_0)} \tag{5}$$

When the geometric correction factor β is approximately equal to unity and the distances r and r' are not significantly different, the spherical-wave reflection coefficient simplifies considerably. Under these conditions, the additional terms accounting for near-field effects and source-image geometry have little influence on the result. Consequently, the reflection coefficient obtained from the spherical-wave model will be very close to that predicted by the plane-wave assumption at normal incidence. This occurs because the propagation behaves almost as if the wavefronts were planar, making the two formulations practically equivalent in terms of magnitude and phase.

Finally, the acoustic absorption coefficient is calculated as follows:

$$\alpha(\theta_0) = 1 - |R(\theta_0)|^2 \; [-] \tag{6}$$

The proposed formulation includes calibration for free field conditions. In fact, the normalized acoustic impedance at a distance r (the distance between the probe and the midpoint between the two microphones) can be expressed as:

$$z_{free,theor} = \frac{1}{\cos(\gamma)} \cdot \frac{1}{1+\frac{j}{kr}} \; [-] \tag{7}$$

After performing the free-field measurement:

$$z_{free,meas} = \frac{1}{\rho c} \cdot \frac{p_{M,free}}{u_{M,free}} \; [-] \tag{8}$$

it is possible to define a calibration function as follows:

$$z_{cal} = \frac{z_{free,theor}}{z_{free,meas}} \; [-] \tag{9}$$

Subsequently, the measurement on the material is corrected as follows:

$$z_M = \frac{1}{\rho c} \cdot \frac{p_M}{u_M} \cdot z_{cal} \; [-] \tag{10}$$

The use of a microphone array makes it possible to simultaneously create several microphone pairs. Specifically, with reference to Figure 2, the following can be constructed:

- 12 pairs with 42 mm spacing (range 2000-5000 Hz);
- 8 pairs with 84 mm spacing (range 300-2000 Hz);
- 4 pairs with 126 mm spacing (range 100-300 Hz).

Frequency ranges have been initially selected based on the indications provided in [1] and subsequently validated through the numerical analysis presented in the following section.

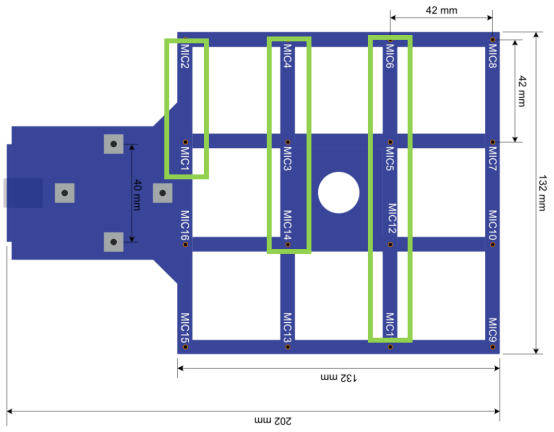

Fig. 2 – Microphone pairs (types of probes are indicated with green boxes) [24]
Coppie microfoniche (le tipologie di sonde sono indicate con i box verdi)

The three types of probes allow measurements to be carried out within appropriate frequency ranges in order to minimize the effect of the finite difference approximation. The frequency ranges used are indicated, in parentheses, in the previous list.

The calculation of the absorption coefficient for all microphone pairs makes it possible to obtain absorption curves as a function of the angle of incidence. The random-incidence absorption, limited to the actual angles of incidence θ_{min} and θ_{max}, computed directly from the geometry of the problem (source–array distance, array–surface distance, array spacings), is calculated as follows:

$$\alpha_{rnd} = \frac{\int_{\theta_{min}}^{\theta_{max}} \alpha(\theta)cos(\theta)sin(\theta)d\theta}{\int_{\theta_{min}}^{\theta_{max}} cos(\theta)sin(\theta)d\theta} \quad (11)$$

2.2 | Measurement set-up and signal processing

The experimental setup was designed to ensure maximum accuracy in measuring acoustic responses and to replicate the conditions required by the proposed method. The configuration includes the following main components:

- 16-channel MEMS microphone array KNOWLES SPH1668LM4H (Minidsp UMA-16 V2 USB [24]) used to acquire acoustic pressures at points distributed in space according to a predefined geometry. This arrangement allows the reconstruction of the sound field and the application of impedance and absorption coefficient calculation procedures.
- FOCUSRITE SCARLETT 4i4 audio interface used for generating the excitation signal.
- Sound source (consisting of a FAITAL 3FA25 3.5 inches loudspeaker and a 3D-printed cabinet) for generating the test signal.
- PRO-JECT STEREO BOX S2 power amplifier required to drive the loudspeaker at the desired sound pressure level, maintaining system linearity and minimizing signal distortion.

In order to minimize the influence of spurious reflections, an exponential sweep was used as the excitation signal. The system responses were processed by convolution with an inverse filter, thus obtaining the impulse responses required for the analysis [25].

A time window was applied to each response in accordance with the specifications given in ISO 13472-1 [20], in order to isolate the contribution of the direct sound and the first reflection and to reduce the effect of residual reflections. Furthermore, in compliance with the same standard, a time-alignment procedure for the direct sound was implemented to correct any phase shifts between the preliminary free-field measurement and the tests carried out on the actual material. Finally, by measuring the time of flight between the direct sound and the reflected sound, it is possible to estimate the distance between the source, the microphone array and the reflection plane.

3 | Results

3.1 | Numerical validation

For an initial numerical validation, a finite element model (FEM) of a poroacoustic material was developed. The model, created using Comsol Multiphysics 6.1 and illustrated in Figure 3, reproduces a simplified configuration for simulating acoustic absorption measurements.

The geometry consists of a cubic volume whose lateral and upper walls are defined as perfectly absorbing, in order to eliminate unwanted reflections and approximate free-field conditions. On the lower surface of the volume lies the sound-absorbing material under analysis, modelled according to the Johnson-Champoux-Allard model [26], which also allows the analytical calculation of the absorption coefficient for comparison with the results of the proposed method. The parameters used for the material were: airflow resistivity σ = 10000 Pa s/m², open porosity σ = 0.99, high frequency limit of tortuosity function α_∞=1.05, viscous characteristic length Λ = 50 μm, thermal characteristic length Λ' = 100 μm and thicknesses equal to 20 and 50 mm. These parameters are representative of commercially available materials (for example, melamine resin, low-density mineral wool, etc.).

Inside the domain, an idealized sound source is positioned, represented by an acoustic monopole, which generates the incident field on the material. Acoustic pressures were extracted at an array of 16 measurement points, arranged according to the actual geometry of the UMA-16 V2 USB mic array system. This configuration allows replication of the experimental setup and provides the data required for estimating impedance and absorption coefficient.

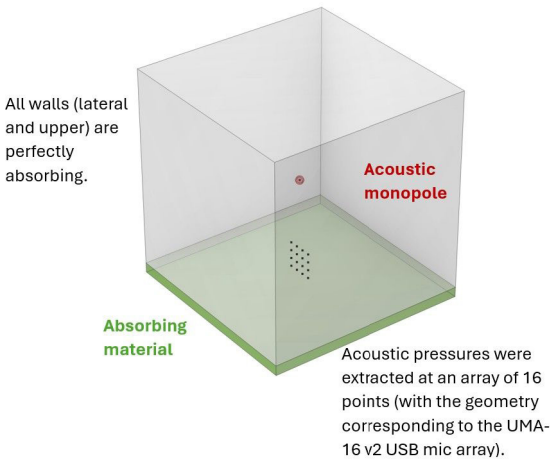

Fig. 3 – Finite element model
Modello agli elementi finiti

Thanks to the absorbing boundary conditions and the controlled source, the model makes it possible to analyse the material's behaviour under ideal conditions, reducing the effects of spurious reflections and providing a solid basis for the numerical validation of the proposed method. Figure 4

shows the comparison between the analytical model and the proposed methodology. From the comparison, a good consistency between the results can be observed.

A structured mesh was used, with the maximum element size determined according to the rule of six elements per wavelength. The analyses were performed over the 80-5600 Hz frequency range, using nine discrete frequencies within each one-third-octave frequency band.

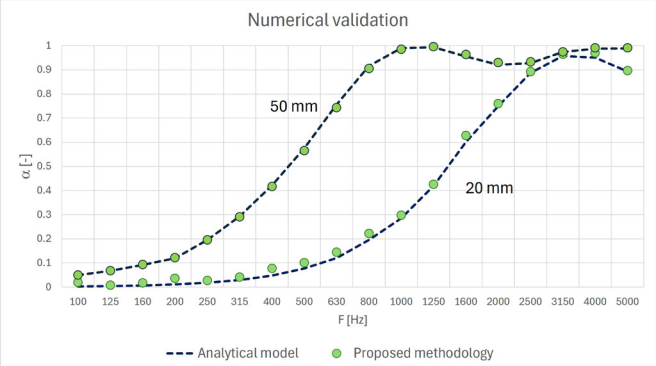

Fig. 4 – Numerical validation of the proposed methodology
Validazione numerica del metodo proposto

3.2 | Experimental validation

For the experimental validation, a measurement campaign was carried out inside an anechoic room, in order to ensure controlled conditions and minimize the effects of spurious reflections. Before testing the materials, the measurement system was calibrated in free field, as shown in Figure 5, by acquiring the impulse responses generated by the sound source. This calibration step is essential to correct any phase shifts and to define the transfer function required for estimating acoustic impedance.

Figure 5 also shows the test performed on a perfectly reflecting surface, used as a reference condition to verify the correctness of the method. This configuration makes it possible to assess the system's ability to distinguish between incident and reflected components, as well as to quantify the accuracy of the time-alignment procedure specified by ISO 13472-1 [20].

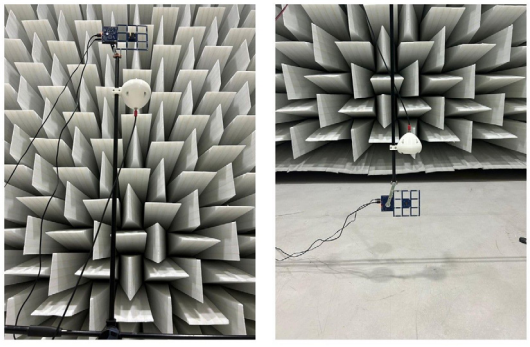

Fig. 5 – (a) Free field calibration. (b) Reflecting surface test
(a) Calibrazione in campo libero. (b) Misura su superficie riflettente

The source was positioned at a distance of 50 cm from the reflecting surface and 20 cm from the microphone array.

Experimental measurements were carried out on materials placed on an acoustically rigid surface (Figure 6) and summarized in Table 2. Material C was also tested in the 0.5 m × 0.5 m format.

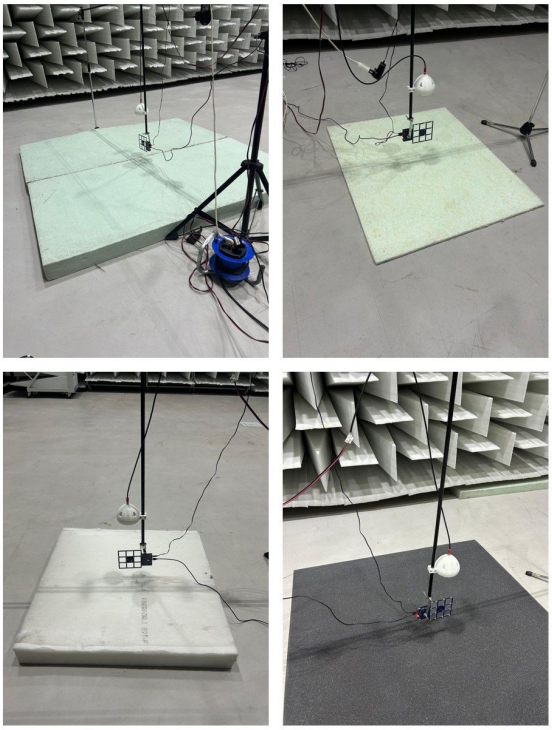

Fig. 6 – Tested materials
Materiali testati

Tab. 2 – Description of tested materials
Descrizione dei materiali testati

	Material	*Density [kg/m³]*	*Thickness [mm]*	*Size [m²]*
A	Polyester fiber	50	100	2 × 2
B	Polyester fiber	50	20	1.2 × 1
C	Polyester fiber	40	120	1 × 1
D	Polyurethane foam	25	50	2 × 2

The acoustic absorption curves (in 1/3 octave bands) for the tested materials are shown in Figure 7.

The results obtained for materials A and C were compared with analytical models based on the Garai-Pompoli model [27], while those related to materials B and D were verified through experimental measurements in accordance with ISO 10534-2 [1].

Figure 7 also shows the results obtained by applying to the 16 microphones a method based on the separation between incident and reflected components (hereafter denoted as Subtraction method), in accordance with the guidelines of ISO 13472-1 [20], which requires free-field calibration and correction on a rigid surface.

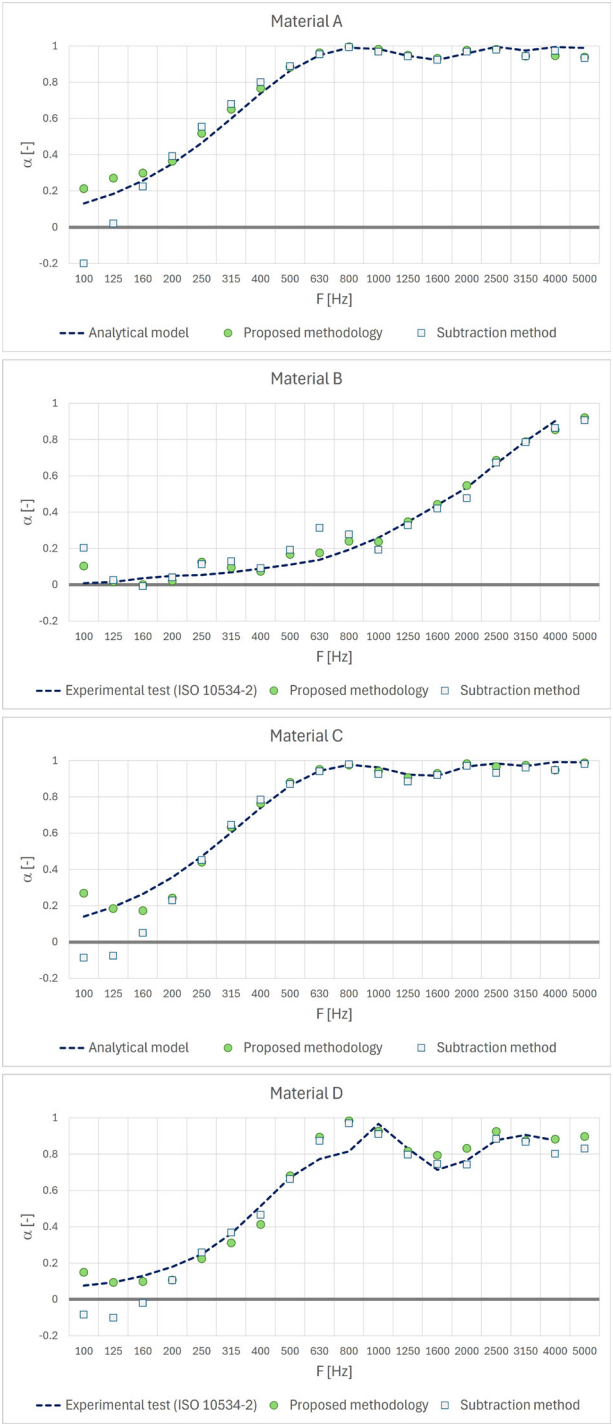

Fig. 7 – Experimental results on tested materials
Risultati sperimentali sui materiali testati

The comparisons show good consistency between the proposed method and the references, although some deviations are observed at low frequencies; however, in this range, the proposed method exhibits improved performance compared to the separation method. The agreement for polyurethane (material D) is less satisfactory (maximum absorption peak shifted), a phenomenon attributable to the compression of the material during the experimental measurement in the impedance tube, which results in stiffening of the material's skeleton.

The average deviation between reference curves and the proposed method ranges between 0.03 and 0.1 for all tested materials. Furthermore, the measurement on material D was repeated 10 times, and maximum deviations of about 0.05 were observed up to a frequency of 200 Hz.

As a demonstration (since the unique absorption coefficient is subsequently calculated using equation 11), Figure 8 shows the absorption coefficients obtained from all microphone pairs for material A. From the comparison, a good consistency among the different measurement points can still be observed, and the frequency limits as a function of the distance between microphones are clearly highlighted.

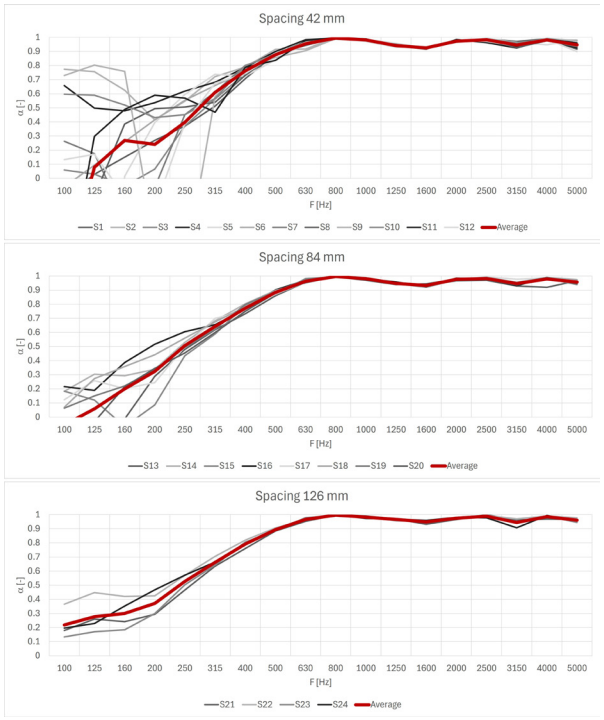

Fig. 8 – Results for individual microphone pairs for material A
Risultati sperimentali per le singole coppie microfoniche per il materiale A

As previously mentioned, material B was tested with two different lateral dimensions, and the comparisons of the measurements obtained with the two samples are shown in Figure 9. Deviation ranging between 0.03 and 0.11 can be observed at lower frequencies, up to 800 Hz.

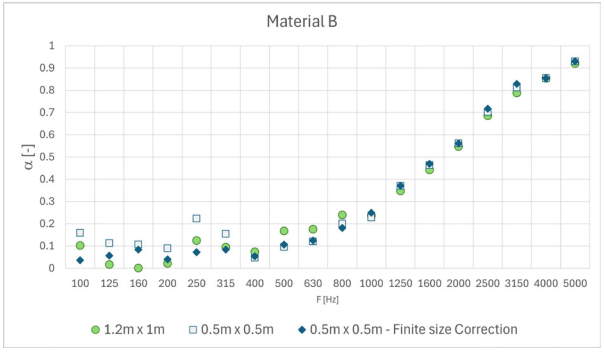

Fig. 9 – Effect of specimen size
Effetto della dimensione del campione

Figure 9 also shows a corrected version of the absorption coefficient of the material with smaller dimensions. The correction was applied as follows. The acoustic absorption coefficient, taking into account the finite size of the panel, requires the use of the radiation impedance $z_R(\theta_0)$ and can be calculated (in accordance with the formulation proposed by Bonfiglio *et al.* [28]), for a given angle θ_0 of incidence, as follows:

$$\alpha_{FS}(\theta_0) = \frac{4\Re\left(z_{M,\infty}(\theta_0)\right)}{\left|z_{M,\infty}(\theta_0)+z_R(\theta_0)\right|^2 \cdot cos(\theta_0)} \quad (12)$$

where $z_{R,\infty}(\theta_0)$ is the surface impedance of an equivalent specimen of infinite size. This surface impedance can be calculated by minimizing the difference, for each angle of incidence and for each frequency of interest, between the absorption coefficient measured using the proposed formulation and that determined by equation (12). Once the surface impedance of the infinite panel is known, the calculation of the reflection coefficient $R_\infty(\theta_0)$ and the corresponding acoustic absorption coefficient $\alpha_\infty(\theta_0)$ follows. The minimization procedure was based on a bounded nonlinear best-fit scheme [29]. A substantial improvement can be observed when comparing the corrected absorption coefficient of small sample with the measurements obtained on the larger panel.

It is important to note that the correction approach presented here is derived from a formulation originally proposed for square panels. In the reference article, the authors describe a method to extend the applicability of the model to rectangular panels; however, no considerations are provided for panels with irregular shapes. In the same article, the authors also provide a detailed analysis of the uncertainties associated with the finite-size correction. Applying their analysis to a panel with dimensions comparable to the one tested in the present work yields estimated errors below 5% at 100 Hz. a value consistent with the data reported in Figure 9.

Measurements on material C were carried out at two different distances of the sound source from the reflecting plane (i.e. 50 cm and 65 cm). The aim of this test was to verify whether increasing the source distance made the edge diffraction effects more evident, a phenomenon that can influence the estimation of the absorption coefficient. For this reason, the panel with the smallest geometric dimensions among those analysed was chosen, as it is more susceptible to such effects. The results are shown in Figure 10. The analysis reveals that the variation between the two configurations is negligible: the average deviation between the absorption coefficients calculated under the two conditions is about 0.02, a value that confirms the robustness of the proposed method with respect to variations in source distance and the presence of edge effects.

Finally, Figure 11 shows the result of the measurement performed on a perfectly reflective surface. From the graph, the presence of residual absorption is noticeable, especially at frequencies below 1000 Hz. These deviations could be the source of measurement uncertainties in the case of materials with a low absorption coefficient.

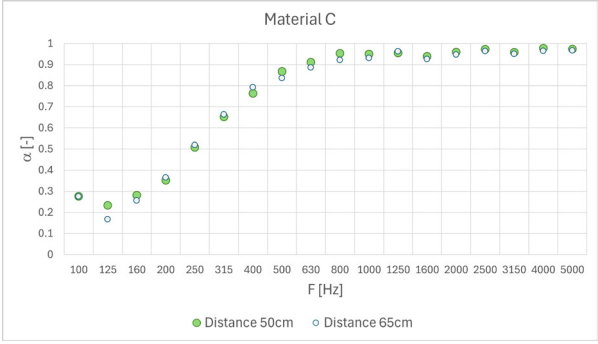

Fig. 10 – Effect of the distance between the source and the reflecting plane for material C

Effetto della distanza tra sorgente e piano riflettente

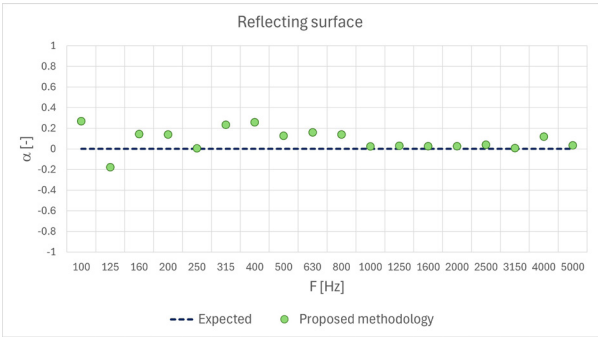

Fig. 11 – Results related to reflecting surface measurement

Risultati relativi alla prova su superficie riflettente

4 | Conclusions

This study introduced and validated an innovative method for measuring the acoustic absorption coefficient under normal incidence conditions directly *in-situ*, based on the use of a low-cost microphone array. This approach is proposed as an alternative to standardized techniques, such as the impedance tube and the reverberation chamber, which, although ensuring high repeatability, present significant limitations when applied in real-world contexts. The developed methodology exploits microphone pairs for the calculation of normalized acoustic impedance and reflection coefficient, integrating a free-field calibration procedure. This strategy allows for reducing operational complexity, extending the range of analysable frequencies (100 Hz-5000 Hz) through the use of differentiated spacers. Furthermore, the proposed configuration enables fast and reliable measurements without resorting to expensive instrumentation or complex setups. Numerical validation activities, carried out through finite element modelling, highlighted good consistency between the method's results and the reference analytical models. Similarly, experimental tests in an anechoic chamber confirmed the robustness of the system with respect to geometric variations, edge effects, and source distance, with average deviations below 0.1. These findings demonstrate the method's ability to provide accurate estimates even under non-ideal operating conditions. Despite the encouraging results, some critical issues

emerged at low frequencies and in the presence of materials with non-linear behaviour, which require further investigation. Looking ahead, the method could be extended to the analysis of oblique incidence and integrated with advanced beamforming techniques and data-driven algorithms, in order to improve spatial resolution and noise robustness. Moreover, the implementation of automated procedures for calibration and signal processing could foster the development of portable solutions, expanding application possibilities in architectural, building, industrial contexts, and for outdoor measurements (asphalt and acoustic barriers).

Conclusioni

Questo studio ha introdotto e validato un metodo innovativo per la misura del coefficiente di assorbimento acustico a incidenza normale direttamente in situ, basato sull'impiego di un array di microfoni a basso costo. L'approccio è proposto come alternativa alle tecniche standardizzate, quali il tubo d'impedenza e la camera riverberante, che, pur garantendo elevata ripetibilità, presentano significative limitazioni in contesti reali. La metodologia sviluppata sfrutta coppie di microfoni per il calcolo dell'impedenza acustica normalizzata e del coefficiente di riflessione, integrando una procedura di calibrazione in campo libero. Tale strategia consente di ridurre la complessità operativa ed estendere l'intervallo di frequenze analizzabili (100 Hz-5000 Hz) mediante l'uso di distanziatori differenziati. Inoltre, la configurazione proposta permette misure rapide e affidabili senza ricorrere a strumentazione costosa o setup complessi. Le attività di validazione numerica, condotte tramite modellazione agli elementi finiti, hanno evidenziato una buona coerenza tra i risultati del metodo e i modelli analitici di riferimento. Analogamente, le prove sperimentali in camera anecoica hanno confermato la robustezza del sistema rispetto a variazioni geometriche, effetti di bordo e distanza della sorgente, con scarti medi inferiori a 0,1. Questi risultati dimostrano la capacità del metodo di fornire stime accurate anche in condizioni operative non ideali. Nonostante gli esiti incoraggianti, sono emerse criticità alle basse frequenze e in presenza di materiali con comportamento non lineare, che richiedono ulteriori approfondimenti. In prospettiva, il metodo potrà essere esteso all'analisi in incidenza obliqua e integrato con tecniche avanzate di beamforming e algoritmi data-driven, al fine di migliorare la risoluzione spaziale e la robustezza al rumore. Inoltre, l'implementazione di procedure automatizzate per calibrazione ed elaborazione del segnale potrà favorire lo sviluppo di soluzioni portatili, ampliando le possibilità applicative in ambito architettonico, edilizio, industriale e per misure outdoor (asfalti e barriere acustiche).

Acknowledgements

The authors would like to thank Dr. Laura Biagi and Dr. Andrea Santoni for their invaluable comments and suggestions, which significantly contributed to the quality of this paper.

References

[1] International Organization for Standardization, ISO 10534-2:2023 – Acoustics – Determination of sound absorption coefficient and impedance in impedance tubes, (2023).

[2] E33 Committee, Test Method for Impedance and Absorption of Acoustical Materials Using a Tube, Two Microphones and a Digital Frequency Analysis System, (n.d.). https://doi.org/10.1520/E1050-19.

[3] International Organization for Standardization, ISO 354:2003 – Acoustics – Measurement of sound absorption in a reverberation room, (2003).

[4] E33 Committee, Test Method for Sound Absorption and Sound Absorption Coefficients by the Reverberation Room Method, (n.d.). https://doi.org/10.1520/C0423-22.

[5] M. Tamura, Spatial Fourier transform method of measuring reflection coefficients at oblique incidence. I: Theory and numerical examples, The Journal of the Acoustical Society of America 88 (1990) 2259–2264. https://doi.org/10.1121/1.400068.

[6] M. Tamura, J.F. Allard, D. Lafarge, Spatial Fourier-transform method for measuring reflection coefficients at oblique incidence. II. Experimental results, The Journal of the Acoustical Society of America 97 (1995) 2255–2262. https://doi.org/10.1121/1.412940.

[7] L. Boeckx, G. Jansens, W. Lauriks, G. Vermeir, The Tamura method, a free field technique for scanning surfaces, in: Proceedings of the Institute of Acoustics, 2003. https://www.ioa.org.uk/system/files/proceedings/l_boeckx_g_jansens_w_lauriks_g_vermeir_the_tamura_method_a_free_field_technique_for_scanning_surfaces.pdf.

[8] H. Aygun, Spatial Fourier transform method to determine reflection and absorption coefficient of porous rigid materials applying Johnson-Champoux-Allard model, in: 2023.

[9] J. Hald, W. Song, K. Haddad, C.-H. Jeong, A. Richard, In-situ impedance and absorption coefficient measurements using a double-layer microphone array, Applied Acoustics 143 (2019) 74–83. https://doi.org/10.1016/j.apacoust.2018.08.027.

[10] A. Paszkiewicz, G. Herold, E. Sarradj, Microphone array measurement for the determination of the absorption coefficient, in: Berlin Beamforming Conference (BeBeC), 2020. https://www.bebec.eu/fileadmin/bebec/downloads/bebec-2020/papers/BeBeC-2020-D31.pdf.

[11] S. Spors, T. Rettberg, On the Estimation of Acoustic Reflection Coefficients from In-Situ Measurements using a Spherical Microphone Array, in: DAGA 2018, 2018. https://pub.dega-akustik.de/DAGA_2018/data/articles/000471.pdf.

[12] S.F. Wu, Techniques for Implementing Near-Field Acoustical Holography, Sound & Vibration Magazine (2010). http://www.sandv.com/downloads/1002wuxx.pdf.

[13] E. Fernandez-Grande, Four decades of near-field acoustic holography, The Journal of the Acoustical Society of America 152 (2022) R1–R2. https://doi.org/10.1121/10.0011806.

[14] Microflown Technologies, In-situ Sound Absorption testing, (2024). https://www.microflown.com/products/acoustic-material-testing/in-situ-absorption.

[15] M. Li, W. Van Keulen, E. Tijs, M. Van De Ven, A. Molenaar, Sound absorption measurement of road surface with in situ technology, Applied Acoustics 88 (2015) 12–21. https://doi.org/10.1016/j.apacoust.2014.07.009.

[16] M. Nosko, E. Tijs, H.-E. de Bree, A study of influences of the in situ surface impedance measurement technique, in: DAGA Proceedings, 2008. https://pub.dega-akustik.de/DAGA_1999-2008/data/articles/003398.pdf.

[17] Y. Takahashi, T. Otsuru, R. Tomiku, In situ measurements of absorption characteristics using two microphones and environmental “anonymous” noise, Acoust. Sci. & Tech. 24 (2003) 382–385. https://doi.org/10.1250/ast.24.382.

[18] N. Okamoto, T. Otsuru, R. Tomiku, K. Ito, In-situ Sound Absorption Measurement Method of Materials Using Ensemble Averaging, in: ICA 2019, 2019. https://pub.dega-akustik.de/ICA2019/data/articles/001305.pdf.

[19] L. Emmerich, P. Aste, E. Brandão, M. Nolan, J. Cuenca, U.P. Svensson, M. Maeder, S. Marburg, E. Zea, A data-driven two-microphone method for *in situ* sound absorption measurements of porous materials, The Journal of the Acoustical Society of America 158 (2025) 1711–1722. https://doi.org/10.1121/10.0039101.

[20] International Organization for Standardization, ISO 13472-1:2022 – Acoustics – Measurement of sound absorption properties of road surfaces in situ – Part 1: Extended surface method, (2022).

[21] International Organization for Standardization, ISO 13472-2:2025 – Acoustics – Measurement of sound absorption properties of road surfaces in situ – Part 2: Spot method for reflective surfaces, (n.d.).

[22] M. Garai, In situ sound absorption coefficient measurement of various surfaces, in: Conference Paper, 2002. https://www.academia.edu/72709462/In_Situ_Sound_Absorption_Coefficient_Measurement_of_Various_Surfaces.

[23] M. Bérengier, M. Garai, A state-of-the-art of in situ measurement of the sound absorption coefficient of road pavements, in: A. Farina (Ed.), Measurement Methods of Acoustical Properties of Materials, 2003. https://www.angelofarina.it/Public/Standing-Wave/4_05.pdf.

[24] M.U.-16 v2 USB, ArrayMiniDSP, (2025). https://www.minidsp.com/products/usb-audio-interface/uma-16-microphone-array.

[25] A. Farina, Simultaneous Measurement of Impulse Response and Distortion with a Swept-Sine Technique, Journal of The Audio Engineering Society (2000). https://api.semanticscholar.org/CorpusID:9614437.

[26] J.F. Allard, N. Atalla, Propagation of Sound in Porous Media: Modelling Sound Absorbing Materials, 1st ed., Wiley, 2009. https://doi.org/10.1002/9780470747339.

[27] M. Garai, F. Pompoli, A simple empirical model of polyester fibre materials for acoustical applications, Applied Acoustics 66 (2005) 1383–1398. https://doi.org/10.1016/j.apacoust.2005.04.008.

[28] P. Bonfiglio, F. Pompoli, R. Lionti, A reduced-order integral formulation to account for the finite size effect of isotropic square panels using the transfer matrix method, The Journal of the Acoustical Society of America 139 (2016) 1773–1783. https://doi.org/10.1121/1.4945717.

[29] J.C. Lagarias, J.A. Reeds, M.H. Wright, P.E. Wright, Convergence Properties of the Nelder--Mead Simplex Method in Low Dimensions, SIAM J. Optim. 9 (1998) 112–147. https://doi.org/10.1137/S1052623496303470.